EXTRA-COLUMN EFFECTS IN DETERMINATION OF RATE PARAMETERS BY THE CHROMATOGRAPHIC METHOD

Olga SOLCOVA[1] and Petr SCHNEIDER[2]

Institute of Chemical Process Fundamentals, Academy of Sciences of the Czech Republic, 165 02 Prague 6-Suchdol, Czech Republic; e-mail: [1] solcova@icpf.cas.cz, [2] schneider@icpf.cas.cz

Received October 27, 1995
Accepted December 27, 1995

It was shown that the sampling loop, detector and connecting elements in the chromatographic set-up for determination of transport parameters by the dynamic method significantly influence the response peaks from columns packed with porous or nonporous particles. A method, based on the use of convolution theorem, was developed which can take these effects into account. The applicability of this method was demonstrated on the case of axial dispersion in a single-pellet-string column (SPSR) packed with nonporous particles. It is possible to handle also responses from columns packed with porous particles by a similar procedure.

Key words: Axial dispersion; Peclet number; Single-pellet-string column; Effective diffusion coefficient.

Chromatographic technique is one of the popular methods for determination of effective diffusion coefficients of gases in porous solids. In this technique the porous particles are packed in a column through which a carrier-gas (C) flows at constant rate. At the column inlet a pulse of another gas (tracer – T) is injected into the carrier stream (T→C). Tracer concentration is monitored at the column outlet by a suitable detector (thermal conductivity, flame ionisation, etc.) and the recorded outlet (response) peak is then analyzed. Several processes occur during the passage of the tracer band through the column: besides convection and axial dispersion, transport of tracer through the laminar film around the packing particles takes place followed by diffusion in the pore structure. Tracer is, then, possibly adsorbed on the internal surface of the packing.

Porous particles can be packed in the column in two ways. Either a wide bed packed with particles is formed – to guarantee the axially dispersed plug flow hydrodynamics it is necessary to have the column diameter to particle diameter ratio larger than about 20. Or, particles are packed one by one into a column with diameter exceeding that of the particles by only 10–20%. This arrangement, known as single-pellet-string column[1] (SPSR), is used usually for spherical or cylindrical porous particles. The advantage of SPSR originates from the requirement of high linear carrier-gas velocities which suppress the tracer peak broadening due to axial dispersion. This is even more significant when inert (nonadsorbable) tracers are used as tracers which move through the column

with the carrier-gas velocity. The use of inert tracers prevents their adsorption and the possible surface diffusion which obscures the effective diffusion coefficients[2].

The analysis of outlet peaks is based on the model of processes in the column. Today the Kubin–Kucera model[3–4] which accounts for all the above mentioned processes, as long as they can be described by linear (differential) equations, is used nearly exclusively. Several possibilities exist to obtain rate parameters of infra-column processes (axial dispersion coefficient, external mass transfer coefficient, effective diffusion coefficient, adsorption/desorption rate constants, adsorption equilibrium constant) from the column response peaks. The moment approach in which the moments of the peaks are matched to theoretical expressions developed from the system of model (partial) differential equations is widespread because of its simplicity[5]. Because of the availability of (personal) computers matching of whole column response peaks with model equations starts to be the predominant analysis method. Such matching can be performed in the Laplace-[6] or Fourier-domain[7], or preferably in the time-domain[8–9].

There is, however, one point that complicates the analysis. The model equations describe correctly the intra-column processes but neglect the effects of processes upstream and downstream of the column (extra column effects – ECE). Thus, peak distortion due to the sampling valve, connections between sampling valve, column and detector and detector itself is not accounted for. This problem arises always when matching of peaks in Laplace-, Fourier- or time-domain is applied. In the moment analysis the situation is simpler because it is possible to subtract the moments of responses with the column removed from the experimental setup, from the column response moments.

It is the aim of this paper to show: (i) the significance of ECE and (ii) to suggest a way for inclusion of these effects into the time-domain matching method of response peak analysis.

The first task was accomplished by obtaining responses of a simple chromatographic system from which the chromatographic column was removed. Two types of thermal conductivity detectors were used together with a six-way sampling valve with three sizes of the sampling loop. Inert gases were used both as carriers and tracers and measurements were made with several carrier-gas flow-rates.

Convolution of ECE response peaks with theoretical expressions for column processes due to injection of Dirac impulse of tracer (impulse response) was verified for the time-domain matching of column response peaks. This approach is illustrated on the case of a SPSR column packed: (i) with nonporous cylindrical pellets where only axial dispersion of the tracer takes place and (ii) with cylindrical porous pellets of an industrial catalyst where pore diffusion takes place in addition to axial dispersion.

EXPERIMENTAL

Argon, hydrogen and nitrogen were used both as tracer-gases (T) and carrier-gases (C). All gases were taken from pressure cylinders. Flow-rates of carrier and tracer gases were regulated with calibrated mass flow-meter controllers. Carrier-gas flow-rates of 30, 90 and 200 cm^3/min were usually used.

The three sampling loops for the six-way gas sampling valve had the following sizes: sampling loop L1: tube i.d. 1 mm, volume 0.273 cm^3; sampling loop L2: tube i.d. 1 mm, volume 0.558 cm^3; sampling loop L3: tube i.d. 3 mm, volume 0.237 cm^3.

The following thermal conductivity detectors (TCD) were used: SD: semidiffusion detector C-15 (Chemoprojekt Satalice, Czech Republic) with cell volume of approximately 3 cm^3, GM: Micro-TCD 10-955 (Gow-Mac Instruments Co., Gillingham, England) with cell volume 20 μl.

SPSR column was made from stainless steel tube (i.d. 6.8 mm, length 49 cm). Cylindrical brass pellets (diameter/length: 5.7 mm/3.8 mm) were used as column packing.

Metal capillaries (i.d. 1 mm) with minimized length were employed for connecting the system components.

The response peaks from the TCD's were fed into a digital data logger (1 000 data points). After zero-line correction (less than 0.1% of the maximum response height) about 50 uniformly distributed points, normalized to the maximum tracer concentration, were retained for further processing. All measurements were at least triplicated. Because of the rapid responses (see below) the positions of maxima of replicated peaks differed slightly (about 0.1–0.2 s). Therefore, the mean maximum position was determined and replicated peaks were shifted to this maximum (Fig. 1*a*). The final response peak (ECE peak) was, then, obtained by averaging the individual responses (Fig. 1*b*).

RESULTS

Extra-Column Effects

Figure 2 shows the effect of different T→C pairs on ECE response peaks (obtained with direct connection between the sampling valve and the SD thermal conductivity

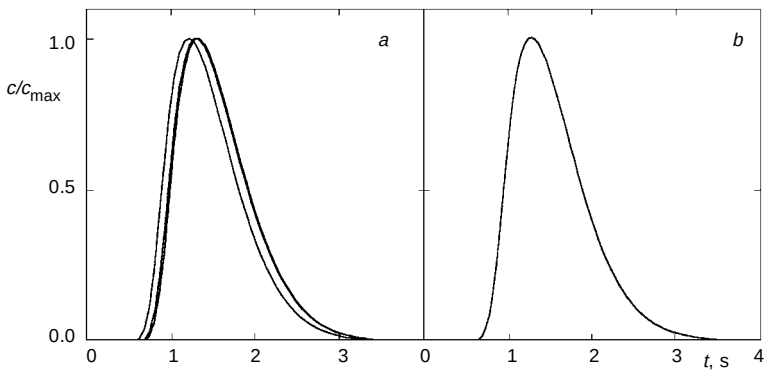

FIG. 1

Replicated ECE peaks (*a*) and the averaged response (*b*). Ar→H_2; carrier flow-rate 90 cm^3/min; sampling loop L1; detector GM

detector. For the light carrier-gas, hydrogen, the ECE peak is shorter than for the heavier nitrogen. The influence of the molecular weight of tracer is somewhat less marked. The carrier-gas flow-rate has a marked effect on the shape of ECE peaks. Figure 3 shows that even with the very high flow-rate (200 cm^3/min) the ECE response needs 3–4 s to vanish. The effect of sampling loop size is illustrated in Fig. 4. A role plays not only the loop volume, as seen from comparison of peaks 1 and 2, but also the loop diameter (cf. peaks 1 and 3). The effect of the detector cell-volume is very pronounced. Figure 5 compares ECE peaks obtained with the small cell-volume detector GM and the large cell-volume semidiffusion TCD, SD. Due to mixing in the detector cell the amount of tailing for the SD detector is much larger than for the GM detector.

Without ECE one would expect the ECE peak as a rectangular signal of width t_0 = (loop volume)/(carrier-gas flow-rate), which appears immediately after injection. That this is not the case for any combination of T→C pairs, flow-rates, sampling loops and detectors is obvious.

Attempts were made to describe the obtained response curves by a simple model taking into account the possible processes from which ECE's originate. Two models were verified:

Model I. An arrangement of sampling loop with gas plug flow, followed by an ideally mixed region and a delaying region again with gas plug flow. This model is characterized by the volume of the ideally mixed zone, V_{mix}, and volume of the delaying zone, V_{del}.

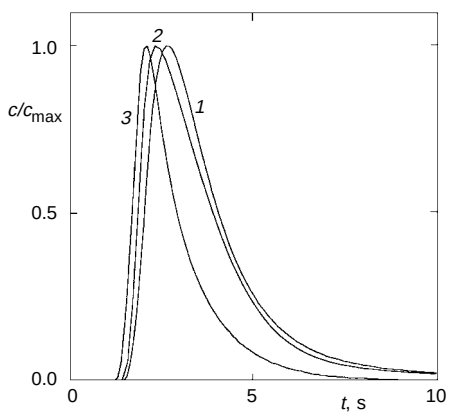

FIG. 2
ECE peaks for different T→C pairs. Carrier flow-rate 30 cm^3/min; sampling loop L1; detector SD; *1* Ar→N_2; *2* H_2→N_2; *3* Ar→H_2

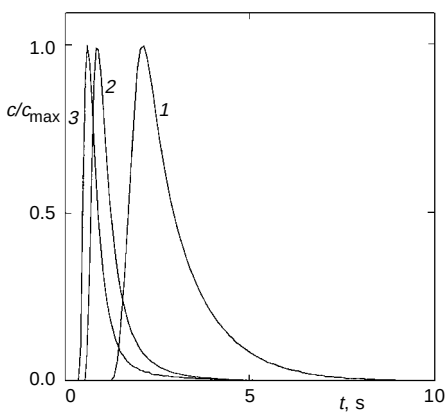

FIG. 3
Influence of carrier-gas flow-rates on ECE peaks. Ar→H_2; sampling loop L1; detector SD; carrier flow-rate: *1* 30 cm^3/min; *2* 90 cm^3/min; *3* 200 cm^3/min

Model II. Similar arrangement as in (I) with addition of a stagnant region in which the tracer exchange depends on the difference between concentrations in the main stream and the stagnant region. The model parameters are: V_{mix}, V_{del}, volume of the stagnant zone, V_{stag}, and the exchange rate constant between the main gas stream and the stagnant volume, k.

The closed form expressions of the time development of tracer concentration for both models, $c_I(t)$ and $c_{II}(t)$, are shown in Appendix 1. The model parameters were determined by matching the experimental ECE response peaks to expressions for $c_I(t)$ and $c_{II}(t)$. The sum of squared differences between the experimental and theoretical response was used as the objective function in minimization performed by the simplex algorithm[10].

The ability of Models I and II to simulate the ECE response peaks is illustrated in Fig. 6. As can be seen the agreement for the five-parameter Model II is better than for the three-parameter Model I. Even with Model II the shape of the simulated curve is slightly different from the experiment; viz the front part of the simulated peak cuts its decreasing part in a sharp angle whereas the experimental peak passes through the maximum monotonously. Obviously, processes that were taken as the basis of both models are oversimplified, or, some additional process was not accounted for. This is clearly demonstrated in Fig. 7 where the optimum Model I parameters, V_{mix} and V_{del}, are plotted for different carrier-gas flow-rates. Both parameters increase with the flow-rate which contradicts the model. The situation is the same also for Model II (not shown). Thus, the suggested models with optimum parameters can be used merely as

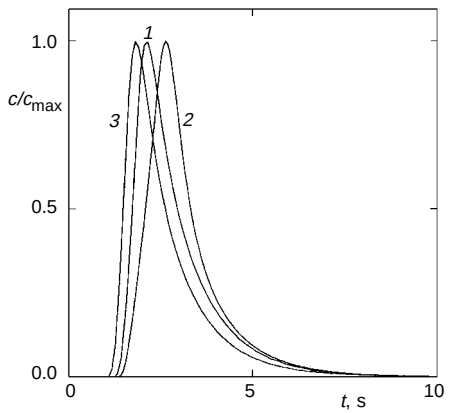

FIG. 4
Effect of sampling loops on ECE peaks. Ar→H_2; carrier flow-rate 30 cm^3/min; detector SD; sampling loop: *1* L1; *2* L2; *3* L3

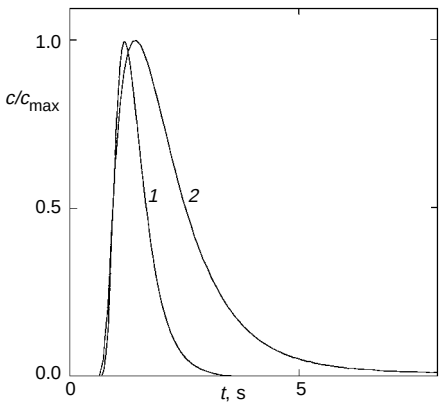

FIG. 5
ECE peaks for different TC detectors. Ar→N_2; carrier flow-rate 90 cm^3/min; sampling loop L1; detector: *1* GM; *2* SD

suitable empirical functions which can reasonably reproduce the experimental responses due to ECE.

Inclusion of ECE to Impulse Response

If the impulse response of a column (i.e. response to a Dirac pulse of tracer) is described by a function $h(t)$, then the column response $c(t)$ is given by the convolution theorem as

$$c(t) = \int_0^t g(t-u)\, h(u)\, \mathrm{d}u \ , \qquad (1)$$

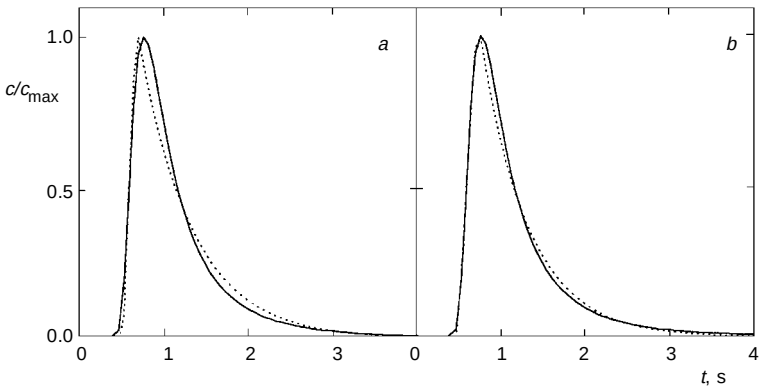

FIG. 6
Comparison of experimental and calculated ECE peaks for Model 1 (*a*) and Model II (*b*). Ar→H_2; carrier flow-rate 90 cm^3/min; sampling loop L3; detector SD. —— Experimental, – – – – calculated

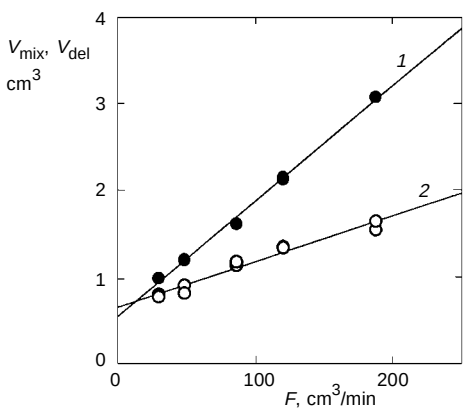

FIG. 7
Fitting parameters for Model I (V_{mix} (*1*), V_{del} (*2*)) for different flow-rates of carrier gas. H_2→N_2; sampling loop L1; detector SD

where $g(t)$ describes the shape of the signal entering the column instead of the Dirac pulse. In linear systems it is immaterial if the ECE are distributed in different places of the system or, if they are concentrated in one place and in what order they are arranged. Therefore, it is possible to use the experimental ECE response peak obtained in the system without the chromatographic column, in place of $g(t)$. Obviously, even when $g(t)$ and $h(t)$ are known in closed form, the integral in Eq. (*1*) can or has to be solved numerically. Because of the not completely satisfactory ECE modelling results presented above it seems simpler to use directly the experimental ECE response peaks. This circumvents the modelling and searching for optimum parameters. We have found that interpolation of ECE response peaks with cubic splines[10] is easier and reproduces the peaks far better.

Inclusion of ECE into Measurements of Axial Dispersion

The application of Eq. (*1*) is demonstrated for the experimental set-up in which a SPSR column packed with nonporous brass cylinders was added. Only axial dispersion causes peak broadening in the SPSR column. The shape of the system response peak is, then, a result of combined ECE effects and column axial dispersion. The impulse response of a column in which only axial disperion plays a role, $h(t)$, is given in Appendix 2. Hence, two parameters are needed for calculation of the system response through Eq. (*1*), viz. the carrier-gas mean residence time, t_c, and the Peclet number, *Pe*.

Figure 8 shows the ECE responses for detector SD and sampling loop L3 and detector GM and sampling loop L1, together with the experimental corresponding column responses. For both detector/sampling loop combinations optimum adjustable parameters t_c and *Pe* were determined with the use of Eq. (*1*). In the first case (SD/L3) t_c = 5.9 s and *Pe* = 167.8; for the second case (GM/L1) t_c = 5.9 s and *Pe* = 164.1, i.e. identical t_c parameters and Peclet numbers differing by about 2% were found in spite of the dif-

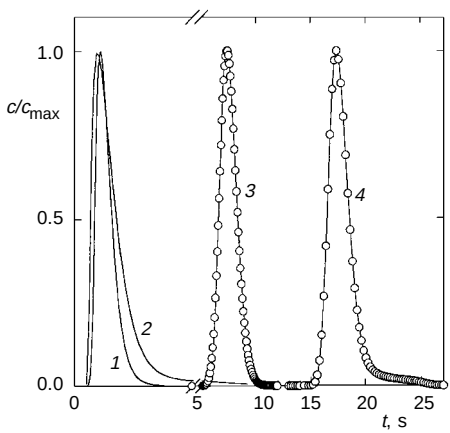

FIG. 8
Comparison of $H_2 \rightarrow N_2$ experimental and calculated responses for SPSR packed with nonporous particle for two combinations of TCD's and sampling loops. Carrier flow-rate 90 cm^3/min. *1* ECE peak: detector/sampling loop: GM/L1; *2* ECE peak: SD/L3; *3* SPSR response: GM/L1; *4* SPSR response: SD/L3 (for clarity shifted 10 s to the right). Lines – experimental, points – calculated

ference in column and ECE peaks. The agreement of column responses calculated with optimum parameters (circles) with the experimental peaks (lines) confirms the physical meaning of these parameters and, thus, the correctness of the method by which the ECE's were included into the system response.

Inclusion of ECE into Measurements of Effective Diffusion Coefficients

Determination of effective diffusion coefficients, D_{TC}, of the pair T→C in the pore structure of pellets packed in the chromatographic column requires that the system response for column packed with porous particles, the response of the identical column packed with nonporous particles of the same shape and size, and the ECE peak for the T→C pair are known. Both responses have to be measured at the same temperature, pressure, carrier flow-rate and with the same sampling loop, detector and connecting elements.

Alternatively, ECE peaks and responses of the column packed with nonporous particles can be used for evaluation of Peclet numbers in the above suggested way separately. An interpolation between the obtained Peclet numbers for the carrier flow-rates used with the column packed with porous particles is, then, necessary.

D_{TC} is determined by matching the response of the column packed with porous particles to Eq. (*1*) with $h(t)$, which is given in Appendix 3 for the Kubin–Kucera model. There are four unknown parameters in $h(u)$, viz., the pellet diffusion time, t_{dif} (which contains D_{TC}), the mean residence time of the carrier-gas in the interparticle space, t_c, *Pe*, and the adsorption parameter, δ_0. The Peclet number is independently acquired from the system response with the column packed with nonporous particles in the way described above, or, from the separately determined dependence of *Pe* on the carrier flow-rate. The adsorption parameter, δ_0, is known from the pellet porosity, β, column void fraction, α, and tracer adsorption equilibrium constant, K_T. Thus, only t_{dif} and t_c

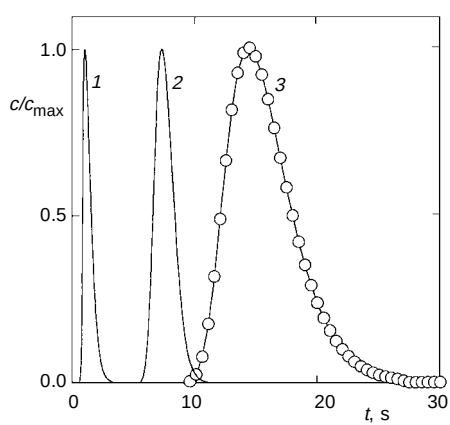

FIG. 9
H_2→N_2 responses of SPSR packed with porous and nonporous pellets; carrier flow-rate 90 cm^3/min. *1* ECE peak; *2* SPSR with nonporous particles; *3* SPSR with porous particles. Lines – experimental, points – calculated with t_c = 8.9 s, *Pe* = 164.1, $\gamma = \delta_0 = 0.5$

have to be obtained by matching. As these parameters are not correlated the matching progress is straighforward. From our experience the simplex algorithm[10] proved to be sufficiently rapid and stable in the matching.

Figure 9 illustrates the results of this procedure for data obtained with a SPSR column packed with cylindrical pellets of a porous industrial catalyst of the same size as non-porous brass pellets used above. For fixed $\gamma = \delta_0 = 0.5$ and $Pe = 164.1$ the adjustable parameters were as follows: $t_c = 8.9$ s and $t_{dif} = 10.1$ s. Circles in Fig. 9 demonstrate the perfect matching of the experimental column response (line) with the simulated results (points).

The financial support by the Grant Agencies of the Czech Republic (Grant No. 104-94-1025) and the Academy of Sciences of the Czech Republic (Grant No. A472408) is thankfully appreciated.

SYMBOLS

c	tracer molar concentration
D_{TC}	effective diffusion coefficient
E	axial dispersion coefficient
F	volumetric flow-rate of carrier-gas
g	tracer input signal
h	tracer impulse response function
k	exchange rate constant between main gas stream and stagnant region
K_T	adsorption equilibrium constant of tracer in pores
L	packed column length
Pe	Peclet number: vL/E
R	radius of spherical packing particle
t	time
t_c	tracer mean residence time in the interparticle space
v	carrier gas linear interstitial velocity
V	volume
α	interstitial column void fraction
β	porosity of porous particle
γ	$(1 - \alpha)\beta/\alpha$
δ_0	adsorption parameter: $\delta_0 = \gamma(1 + K_T)$
κ	relative exchange rate constant

Subscripts

c	for column
dif	for pore diffusion
del	for the delaying region
stag	for the stagnant region
mix	for the region completely mixed region
0	for sampling loop

APPENDIX 1

Model I

$$c_I/H = 0 \qquad \text{for } 0 < t < t_{del}$$

$$c_I/H = 1 - \exp\left[-(t - t_{del})/t_{mix}\right] \qquad \text{for } t_{del} < t < t_0 + t_{del}$$

$$c_I/H = \exp\left[-(t - t_0 - t_{del})/t_{mix}\right] - \exp\left[-(t - t_{del})/t_{mix}\right] \qquad \text{for } t > t_0 + t_{del}$$

The tracer residence time in the sampling loop of volume V_0 equals $t_0 = F/V_0$ where F denotes the carrier volumetric flow-rate. Similarly, the residence times in the ideally mixed region (volume V_{mix}) and in the delaying region (volume V_{del}) are: $t_{mix} = F/V_{mix}$, $t_{del} = F/V_{del}$. c^0 is the height of the square wave input pulse of duration t_0. H is a time-independent normalization constant which follows from the requirement that the area below the response signal equals the amount of tracer injected:

$$c^0 t_0 = \int_0^\infty c(t)\, \mathrm{d}t \ .$$

However, it is easier to obtain this constant by matchning the concentration at the simulated peak maximum to the maximum concentration of the experimental peak.

Model II

$$c_{II}/H = 0 \qquad \text{for } t < t_{del}$$

$$c_{II}/H = \frac{1 - (\kappa_{stag}/b_1)}{b_2 - b_1}\left\{\exp\left[-b_1(t - t_{del})\right] - 1\right\} + \frac{1 - (\kappa_{stag}/b_2)}{b_1 - b_2}\left\{\exp\left[-b_2(t - t_{del})\right] - 1\right\}$$

$$\text{for } t_{del} < t < t_{del} + t_0$$

$$c_{II}/H = \frac{1-(\kappa_{stag}/b_1)}{b_2-b_1}\{\exp[-b_1(t-t_{del})] - \exp[-b_1(t-t_{del}-t_0)]\} +$$

$$+ \frac{1-(\kappa_{stag}/b_2)}{b_1-b_2}\{\exp[-b_2(t-t_{del})] - \exp[-b_2(t-t_{del}-t_0)]\}$$

$$\text{for } t > t_0 + t_{del}$$

In the above equations b_1 and b_2 are roots of the quadratic equation

$$b_{1,2} = (1/2[t_{mix} + \kappa_{mix} + \kappa_{stag} \pm \sqrt{[(t_{mix} + \kappa_{mix} + \kappa_{stag})^2 - 4t_{mix}\kappa_{stag}]}$$

with $\kappa_{stag} = k/V_{stag}$, $\kappa_{mix} = k/V_{mix}$, $t_{mix} = F/V_{mix}$. The value k is the exchange rate constant between the main gas stream and the stagnant (unmixed) volume V_{stag}. For the time-independent normalization constant, H, applies the same as for Model I.

APPENDIX 2

Impulse response, $h(t)$, of a packed column in which only axial dispersion causes spreading of a tracer peak is given by Himmelblau and Bischoff[11] in the form

$$h(t) = H\sqrt{\frac{t_C}{t}}\exp\left[-\frac{t_C Pe}{4t}\left(1-\frac{t}{t_C}\right)^2\right].$$

Here t_c is the tracer residence time in the packed column ($t_c = V_c/F$ with column free volume, V_c) and the Peclet number is defined as $Pe = vL/E$ with the carrier-gas linear interstitial velocity, v, column length, L, and axial dispersion coefficient, E. The same arguments as for Model I (Appendix 1) apply for the time-independent normalization constant, H.

APPENDIX 3

For the T→C system the impulse response of a column packed with porous spherical particles of radius, R, in which intraparticle diffusion characterized by an effective diffusion coefficient D_{TC} takes place is given by[12]

$$h(t) = H\int_0^\infty \exp\left(\frac{Pe}{2} - f_1\right)\cos\left(\frac{2\gamma\lambda^2 t}{\delta_0 t_{dif}} - f_2\right)\lambda\, d\lambda$$

with

$$f_{1,2} = \sqrt{\frac{\sqrt{A^2 + B^2} \pm A}{2}}$$

$$A = Pe\left(\frac{Pe}{4} + \frac{3\gamma H_1 t_c}{t_{dif}}\right)$$

$$B = Pe\,\frac{t_c}{t_{dif}}\left(\frac{2\gamma\lambda^2}{\delta_0} + 3\gamma H_2\right)$$

$$H_1 = \lambda\,\frac{\sinh(2\lambda) + \sin(2\lambda)}{\cosh(2\lambda) - \cos(2\gamma)} - 1$$

$$H_2 = \lambda\,\frac{\sinh(2\lambda) - \sin(2\lambda)}{\cosh(2\lambda) - \cos(2\gamma)}\ .$$

t_c is the mean residence time of tracer in the column of length L, Pe is the Peclet number, t_{dif} denotes the diffusion time of the tracer in the pore structure of a pellet, $t_{dif} = R^2\beta/D_{TC}$, δ_0 is the tracer adsorption parameter $\delta_0 = \gamma(1 + K_T)$, and $\gamma = \beta(1 - \alpha)/\alpha$. β is the pellet porosity and α is the column void fraction (interstitial void volume/column volume). Thus, γ, is the pore volume per unit interstitial volume. For an inert tracer ($K_T = 0$): $\delta_0 = \gamma$. The same arguments as for Model I (Appendix 1) apply for the time-independent normalization constant, H.

This equation takes into account equilibrium adsorption of the tracer in the linear region of the adsorption isotherm (adsorption coeffient K_T; for an inert tracer $K_T = 0$) and assumes no transport resistance between the bulk stream and the external surface of porous pellets.

REFERENCES

1. Scott D. S., Lee W., Papa J.: Chem. Eng. Sci. *29*, 2155 (1974).
2. Schneider P., Smith J. M.: AIChE J. *14*, 886 (1968).
3. Kubin M.: Collect. Czech. Chem. Commun. *30*, 1104, 2900 (1965).
4. Kucera E.: J. Chromatogr. *19*, 237 (1965).
5. Schneider P., Smith J. M.: AIChE J. *14*, 237 (1968).
6. Kamiyanagi K., Furusaki S.: Int. Chem. Eng. *25*, 301 (1985).
7. Zygourakis K., Moudgalya K.: Chem. Eng. Commun. *61*, 107 (1987).
8. Fahim M. A., Wakao N.: Chem. Eng. J. *25*, 1 (1982).
9. Wakao N., Kaguei S., Smith J. M.: J. Chem. Eng. Jpn. *12*, 481 (1979).
10. Press W. H., Flannery B. P., Teukolsky S. A., Vetterling W. A.: *Numerical Recipes*. Wiley, New York 1986.
11. Himmelblau D. M., Bischoff K. B.: *Process Analysis and Simulation*. Wiley, New York 1968.
12. Schneider P.: Chem. Eng. Sci. *39*, 927 (1984).